JACS
JOURNAL OF THE AMERICAN CHEMICAL SOCIETY

COMMUNICATION

pubs.acs.org/JACS

# Monitoring Structural Transitions in Icosahedral Virus Protein Cages by Site-Directed Spin Labeling

Robert J. Usselman,[†,§] Eric D. Walter,[†] Debbie Willits,[‡,§] Trevor Douglas,[†,§] Mark Young,[‡,§] and David J. Singel*[,†,§]

[†]Department of Chemistry and Biochemistry, [‡]Department of Plant Sciences and Plant Pathology, and
[§]Center for Bio-Inspired Nanomaterials, Montana State University, Bozeman, Montana 59717, United States

Supporting Information

**ABSTRACT:** This work describes an approach for calculating and measuring dipolar interactions in multispin systems to monitor conformational changes in icosahedral protein cages using site-directed spin labeling. Cowpea chlorotic mottle virus (CCMV) is used as a template that undergoes a pH-dependent reversible capsid expansion wherein the protein cage swells by 10%. The sequence-position-dependent geometric presentation of attached spin-label groups provides a strategy for targeting amino acid residues most probative of structural change. The labeled protein cage residues and structural transition were found to affect the local mobility and dipolar interactions of the spin label, respectively. Line-shape changes provided a spectral signature that could be used to follow the conformational change in CCMV coat dynamics. The results provide evidence for a concerted swelling process in which the cages exist in only two structural forms, with essentially no intermediates. This methodology can be generalized for all symmetry types of icosahedral protein architectures to monitor protein cage dynamics.

Virus protein dynamics are inherently important for assembly, nucleic acid storage and release, and disassembly pathways in the viral life cycle. The ability to monitor icosahedral viral particle conformational changes and structural transitions is required for understanding of chemical environments that affect protein coat dynamics. Here, Cowpea chlorotic mottle virus (CCMV) was used as a model template for monitoring global viral particle dynamics by site-directed spin labeling (SDSL). CCMV undergoes a reversible swelling structural transition between closed and open conformations.[1] A high-resolution crystal structure (3.2 Å) exists for the closed particle, and an cryo-electron microscopy (cryo-EM) image reconstruction is available for the swollen form.[2,3] These structural models give insight for evaluating virus coat dynamics and provide a vantage point for experimental design of spin-label sites. Specific labeled sites separated by different distances in the two structural forms can provide an electron paramagnetic resonance (EPR) spectral contrast. General strategies for the application of SDSL-EPR in the study of macromolecular assemblies exemplified by CCMV are described. These results elucidate directions for future studies of icosahedral cage assembly, disassembly, and conformational changes.

CCMV is a 28 nm spherical RNA plant virus and a member of the Bromoviridae family. The properties of this simple icosahedral virus have been extensively studied, and the protein shell architecture is one focus for the development of hybrid nanocages.[4] The virus protein cage is composed of 180 chemically identical protein subunits with 190 amino acids. The protein subunit is folded into an eight-stranded $\beta$-barrel core with N- and C-termini that extend out to form inter- and intracapsomere contacts. The capsomers, occurring as 12 pentamers and 20 hexamers, self-assemble into $T = 3$ quasi-symmetrical virus particles. The conformational change is thought to occur from carboxyl−carboxyl electrostatic repulsions at the pseudo-threefold axes and is dependent on ionic strength, pH, and divalent metal cations.[2] In the absence of divalent metal ions, varying the pH allows swelling to occur; this process is termed "gating". CCMV gating involves the close-packed icosahedral structure, in which the cage has an outer diameter of ∼28.6 nm at a thickness of ∼25 Å. The open structure contains 60 pores with widths of ∼20 Å and has an overall diameter of ∼31 nm. At low ionic strength ($I < 0.4$), an abrupt pH-controlled swelling is observed at pH ∼7.0, leading to an open conformation. The transition between the two structural forms has been explored previously,[5] but without means to detect intermediate structural states.

SDSL-EPR is a proven technique for studying the structure and dynamics of biological macromolecules.[6] In typical applications, single spin labels are attached to the macromolecule and motional dynamics or solute accessibility is monitored as a function of sequence position. Magnetic dipolar interactions between pairs of spin labels on a protein are accurate for determining distances and distance distributions between pairs of labels. In addition to pulsed EPR techniques for direct measurement of dipolar couplings hidden in a broad EPR line width,[7] there are numerous simple continuous-wave (CW) approaches that are applicable for determining dipolar broadening in the EPR spectrum. These approaches involve analysis of peak-height ratios, detailed simulations, convolution, and deconvolution.[6]

Most SDSL investigations use pairs of labeled sites to determine distances between the labels. In extensions of this methodology beyond two interacting spin labels, dipolar broadening simulations were developed to model the many simultaneously interacting spins on spin-labeled dendrimers.[8] Icosahedral virus cages are ideal systems that satisfy multispin system experimental requirements for monitoring structural changes in fluid solutions via dipolar broadening.[9] The CCMV capsid has a rotational correlation time of ∼5 $\mu$s, which is sufficiently long to avoid averaged-out dipolar interactions. We calculated the dipolar broadening in both the closed and open CCMV forms to choose spin-labeling sites. This calculation allowed for the selection of sites that confer a relatively large difference in line broadening for the open and closed states.

CCMV crystallographic coordinates for the closed model and cryo-EM coordinates for model D were obtained from the VIPER Web site.[10] N-terminal residues 1−26 were not modeled in the

**Received:** August 24, 2010
**Published:** March 09, 2011





dx.doi.org/10.1021/ja107650c | J. Am. Chem. Soc. 2011, 133, 4156–4159

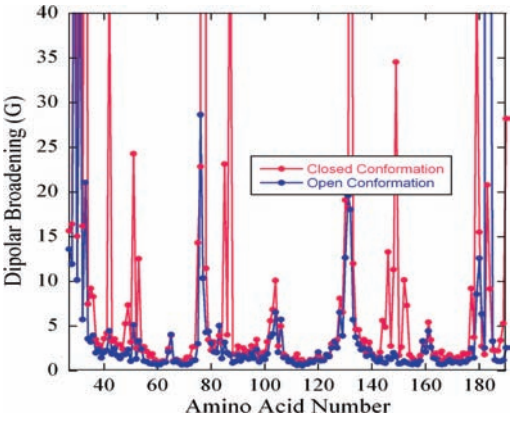


**Figure 1.** Calculated DLBF line widths for each amino acid in the CCMV open and closed model D.

crystal structure and were not used in the dipolar line broadening function (DLBF) calculations. The coordinates were used to calculate pair correlation functions (PCFs) of each amino acid in the subunit sequence for all 180 subunits in the entire capsid. A PCF is a pairwise histogram of all individual intersubunit distances for each amino acid in the CCMV capsid. The PCF for a monomeric particle with $T = 3$ symmetry lends itself to only three definitive distance distributions for a given amino acid residue, while the remaining subunits/residues are spatially identical. DLBFs were calculated from A, B, and C subunit histogram distance distributions for each amino acid end atom in the sequence for the open and closed models using eqs 1−4 in the Supporting Information (SI). The full widths at half height for the DLBFs are shown in Figure 1.

The potential labeling sites arise from amino acids that exhibit large differences in the DLBF for the open and closed conformational states. Dipolar broadening would propagate that change in the EPR spectra and thus give a spectral contrast between open and closed CCMV conformational states. The DLBF calculation for the open and closed states showed drastic changes for certain sites in the amino acid sequence. Most amino acids are spatially arranged such that they exhibit no difference in the DLBF for the two conformational states, indicating that the amino acid distances do not change within the nominal spectral resolution (8−25 Å).

For wild-type (WT) CCMV, a specific amino acid residue of a given particle has 180 potential label sites. There are two native cysteines (59 and 108) located in each monomer. C108 is completely buried and does not react with spin label. C59 is located on the surface of the capsid and is reactive toward maleimide spin labels[11,12] and fluorophores.[13] The C59 intersubunit distances in the quaternary structure are nearly spatially maximized between subunits. The average distance to the nearest neighbor in the closed and open models are 28.5 and 31.6 Å, respectively. The C59 EPR spectrum exhibits fast tethering mobility with a rotational correlation time of $\tau_c \approx 5$ ns; however, contributions from weak dipolar interactions were not used in the simulation.[14] The open (pH 7.4) and closed (pH 6.5) conformational states show a small but discernible change in the EPR spectrum upon pH increase for spin-labeled C59 (Figure 2). The line broadening is slightly larger for C59 in the closed conformation, with a calculated difference of 0.4 *G* (1.3 *G* closed − 0.9 *G* open). A DLBF convolution with the open spectrum yielded a line width of $0.5 \pm 0.3$ *G*, which is in good agreement at the low-resolution end and presumably results from weak dipolar interactions.

For SDSL of CCMV, the mutation sites were chosen on the basis of residues that would give a spectral contrast between

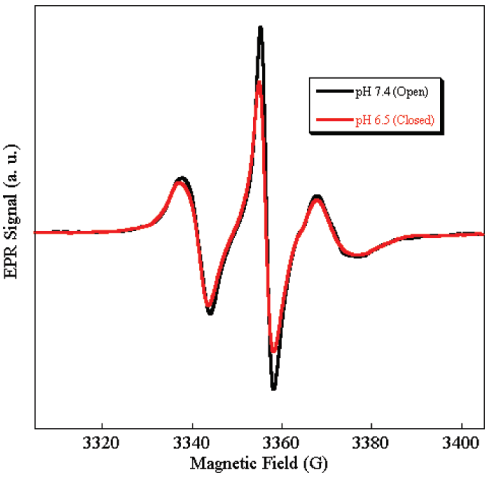


**Figure 2.** EPR spectra of WT CCMV in the open and closed states at 298 K. The experimental spectral contrast, determined by convolution of the open spectrum and a DLBF, is $0.5 \pm 0.3$ *G*.

CCMV conformational states. The pseudo-threefold axes located at the ABC interfaces undergo the most obvious structural changes. All mutation experiments included the native cysteines within the protein coat. The native cysteines are conserved in the Bromovirus sequences and are required for CCMV capsid stability. The DLBF calculations did not include C59 or C108 in the generation of PCFs, and they were not included in calculations for the DLBF map. C59 can be potentially spin-labeled in these mutation experiments, and it is noted that the DLBF calculations would be slightly different in this case. Furthermore, certain spin-labeled mutants show decreased stability in the virus capsid, as determined by mobile peaks that appear the EPR spectra. Therefore, the K42R mutant, a salt-stable (SS) form of CCMV that exhibits enhanced local interactions allowing for global stabilization of CCMV, was used in the SDSL CCMV experiments. This particular mutant was shown to have gating properties identical to those of WT-CCMV.[15,16]

Analogues were constructed with cysteine substitutions at the threefold axes and at dimer contact points. In Figure 3, the difference in broadening for the mutants has been accentuated by normalization of the spectra to have equal areas. The qualitative trend in dipolar line broadening for the closed conformation is in excellent agreement with that from the DLBF calculation but smaller in magnitude. SS-Q149C shows the largest line broadening, with decreasing broadening for SS-A152C, SS-D153C, SS-T181C, and WT-C59. The line widths of the spin-labeled mutants illustrate the spectral contrast needed for monitoring of intermediate states between the open and closed forms. This spectral contrast can be used during a pH titration experiment to follow intermediate structural transition states.

Alanine 152 is relatively exposed at the exterior surface of the pseudo-threefold axis and undergoes a distance change of ∼14 Å (25 Å open − 11.3 Å closed). Residues positioned at the pseudo-threefold axes result in 60 triangular clusters. A pH titration curve for SS-A152C in the pH range 6.9−7.55 is shown in Figure 4. The experimental line broadening difference for open and closed spectra is $3 \pm 1$ *G*, which is lower than the calculated DLBF of ∼9.0 *G* (10.1 *G* closed − 1.1 *G* open). When the dipolar calculation includes the C59 doubly labeled capsid, the resulting DLBF is 4.5 *G*. The combination of proximate and distant labels within the dipolar window lowers the calculated dipolar broadening for the threefold axis sites. The overall broadening could be even lower if more C59


dx.doi.org/10.1021/ja107650c | *J. Am. Chem. Soc.* 2011, 133, 4156–4159

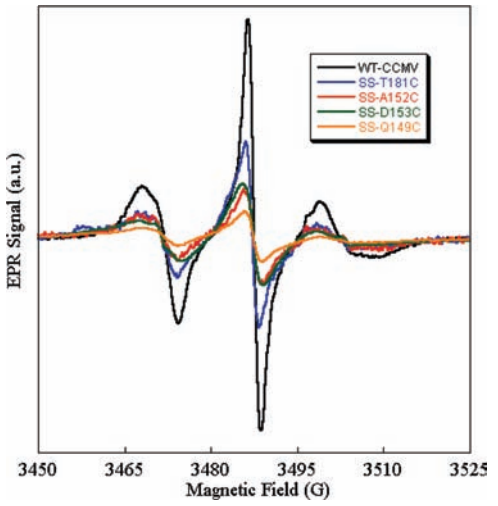


**Figure 3.** EPR spectra of spin-labeled WT CCMV and mutants in the closed conformation at pH 6.5 and 298 K.

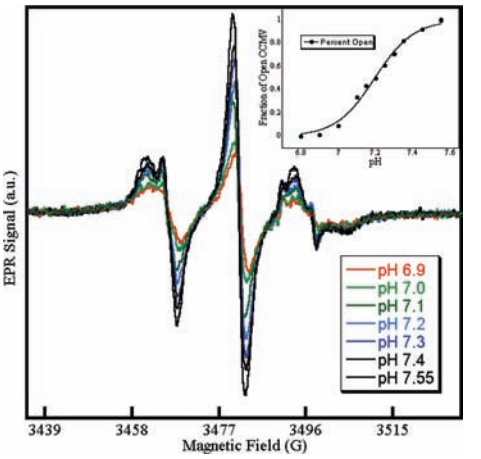


**Figure 4.** pH-titration EPR spectra of SS-A152C CCMV at 298 K. (Inset) Fraction of open CCMV capsids vs pH. The fit used the Nernst equation with $pK_a = 7.2$.

sites are spin-labeled than A152C. Indeed, mass spectrometry indicated doubly labeled subunits of these samples (data not shown).

The EPR spectrum did not change in the pH range 6.3−6.9, consistent with a closed virus particle. For pH 7.0−7.55, the EPR spectrum became narrower with extra sharp features that appeared at pH >7.0. The sharp features indicate the presence of a spin label with a shorter rotational correlation time and suggest that dimer subunits begin to detach from the protein cage. Capsid swelling at elevated pHs could shift the equilibrium to favor the formation of dimers, which implies a possible capsid disassembly route.[17,18] It is worth noting that the formation of a mobile peak at elevated pHs was reversible, and the peak disappeared when the pH was lowered again. Moreover, the narrowed spectrum (open cage) exhibited hysteresis as the pH was lowered and conforms to the closed spectrum at ∼pH 6.5 (data not shown). Disassembly and assembly pathways could be monitored by choosing sites that involve specific pathway changes in the dipolar interactions and rotational correlation times with the concomitant dimer mobile spectrum (see the SI).

The SS-A152C spin-labeled pH titration intermediate spectra were fit with a two-state model. The allosteric behavior of two quaternary states can be explained by two criteria: (a) basis states (two limiting cases) with isosbestic points for the intermediate pH range and (b) intermediate states fit as linear combinations of the basis states. The two basis states in this case would be limiting EPR spectra of the closed (pH <6.9) and open (pH 7.55) conformations. The percentages of the two basis states were fit to each intermediate spectrum in the pH titration curve. The model shows that each point along the curve contains a certain percentage of each basis state (Figure 4 inset). For example, the pH 7.2 spectrum was calculated as 54% open capsids and 46% closed capsids (see the SI). The narrow components notably do not follow a two-state model.

The T181C mutant is unique compared with the other mutation residues because it favors broadening in the open conformation (3.6 *G*). The residues become closer as the virus capsid swells. This residue is located on the CT α-helix, which is responsible for dimer stabilization.[2,3] T181 residues are exposed on the interior of the CCMV protein cage and arranged in a pairwise fashion around the threefold axis. The spin-labeled SS-T181C mutant exhibited broader features than WT-CCMV and SS-A152C. The broad features resemble a powder-pattern line shape and are indicative of relatively more immobilized spin labels. The pH 6.6−7.6 titration curve displayed no EPR spectral changes, which implies this particular site does not change during virus gating (Figure 5). This result is consistent with a strong dimer contact for a closed structure but not dimer contact tightening during capsid expansion, as indicated from the swollen model.[3,19]

The goal of this work was to monitor CCMV conformational changes by SDSL-EPR with the specific objective of probing for the presence or absence of structural intermediates in the course of the pH titration. This required a target sequence position for site-directed labeling and the development of a strategy for target selection. The strategy was to exploit changes in distances, and hence dipolar coupling, among the spin labels to monitor structural transitions. These couplings are readily predicted from the structural models available for CCMV, as shown in Figure 1. While this illustration provides an immediate insight into target sequence positions likely to be probative in the structural transition, the limitations of the prediction need to be highlighted. First, the predictions are only as good as the structural models of the protein, and inherent errors would be most prominent for strongly dipolar coupled spins. In other words, small distance changes would cause large changes in the DLBF. Furthermore, the effects of the cysteine substitution on the conformation, or the range of conformations, adopted by the label were not modeled. The prediction is inherently only semiquantitative.

An indication of the quality of the prediction can be appreciated from our result for the series of mutants near the pseudo-threefold axis. Although this series compared SS mutants with WT CCMV, the qualitative trends followed the expected line broadening calculations (Figure 3). The correlation was excellent, although the expected calculations did not precisely match. This mismatch is most likely caused by the distribution of spin-label conformations that mitigates the broadening and weak dipolar contributions from C59-labeled sites. In addition, the position-dependent spectral contrast, as determined by the different mobility and distance of the labels, could obscure actual line broadening.

More generally, the spectral changes induced by mobilization or demobilization of the label may augment or diminish changes associated with dipolar couplings. Thus, the utility of DLBF predictions for the selection of mutation targets is best when surface residues are selected. In principle, the dipolar versus mobility-related line width effects could be distinguished by conducting the spectroscopy in frozen solution. Unfortunately, this option has the disadvantage of nonbiological conditions and

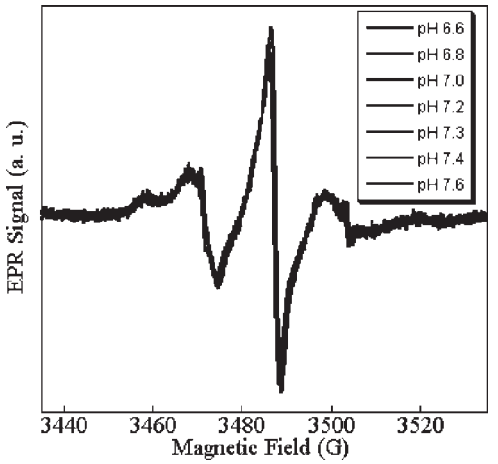


**Figure 5.** pH-titration EPR spectra of spin-labeled SS-T181C CCMV at 298 K. No dipolar-induced changes in the EPR spectra were observed.

requires an investigation of how freezing affects the protein structure and aggregation. In contrast, when SDSL EPR is used as a probe to monitor structural changes, it is not as important to fully understand the origin of the spectral changes as it is simply to track the spectral changes. Moreover, no theory to simultaneously account for label mobility and dipolar broadening exists.[9]

Labeling C59 gave rise to, at best, a modest pH-dependent spectral change (Figure 2). The limited change in the EPR spectra can be rationalized by the remoteness of the labels on the cage in the two structural models and is consistent with the DLBF predictions. Indeed, this result is what ultimately motivated the calculation to search for more probative labeling positions. The plan, however cleverly crafted from a spectroscopic perspective, must ultimately confront the molecular biology of cage assembly and stability. A number of the mutants led to cages that tended to disassemble, as judged by the emergence of a sharp-line (high-mobility) EPR spectrum similar in appearance to a dimer spectrum. Thus, an SS mutant having enhanced global stability and known to undergo the same structural transition was used.[16]

Spin-labeled SS-A152C gave the best supportive evidence for a highly cooperative (two-state) model of the structural transition (Figure 4). The experimental spectra determined as a function of pH showed clear variations that were nicely summarized as linear combinations of the spectra at the limiting pH values; no additional spectral components indicative of intermediates had to be added at intermediate pH values. While this observation cannot prove the absence of intermediate structural states, any such state must either be few in number (consistent with strong cooperativity) or accidentally have EPR spectra identical to that of a basis state. In this light, the most plausible interpretation of the results points to a highly cooperative structural transition.

The T181C mutant showed in no change in the EPR spectra as a function of pH, in contradiction to a predicted contrast (Figure 5). For this mutant, the amino acids are predicted to become closer upon swelling. The rigid limit components in the spectrum may obscure the line broadening.

Collectively, these results illustrate the utility and limits of DLBF calculations for extraction of accurate distances and structural changes in the CCMV protein cage. This methodology provides intriguing results for SDSL-EPR as a probe of pH instability of certain mutants as well as subunit dimers, which is of interest in monitoring of assembly and disassembly processes. SDSL is a unique method for studying structural transitions and subunit dynamics in CCMV at atomic resolution and can be applied to other viral icosahedral protein cages, heat-shock proteins,[20] and ferritins as well as other highly symmetric protein structures such as amlyoid plaques.[21] Furthermore, changing the CCMV structural stability and gating mechanism could be useful as drug delivery vessels.

SDSL CCMV has been shown to be a sensitive method for spectroscopically observing conformational changes in the CCMV protein cage. The spin-labeled virus capsid displayed changes in label mobility and dipolar interactions that were dependent on the residue labeled and pH-induced structural changes, respectively. While isolation of these competing effects was not necessary for qualitative observation of structural changes, it will be important for future investigations to determine interspin distances. The structural transition of CCMV has been shown to have a highly cooperative allosteric structural transition in which only two conformational states exist.

## ■ ASSOCIATED CONTENT

**Supporting Information.** Additional figures and experimental procedures. This material is available free of charge via the Internet at http://pubs.acs.org.

## ■ AUTHOR INFORMATION

**Corresponding Author**
dsingel@chemistry.montana.edu

## ■ ACKNOWLEDGMENT

R.J.U. acknowledges support from the NSF-IGERT Fellowship. This work is supported by the NSF-NIRT Grant No. 0210915. R.J.U. thanks Christian Altenbach for LabVIEW assistance.

## ■ REFERENCES

(1) Bancroft, J. B.; Hiebert, E.; Rees, M. W.; Markham, R. *Virology* **1968**, *34*, 224.
(2) Speir, J. A.; Munshi, S.; Wang, G.; Baker, T. S.; Johnson, J. E. *Structure* **1995**, *3*, 63.
(3) Liu, H.; Qu, C.; Johnson, J. E.; Case, D. A. *J. Struct. Biol.* **2003**, *142*, 356.
(4) Douglas, T.; Young, M. *Science* **2006**, *312*, 873.
(5) Tama, F.; Brooks, C. L., III. *J. Mol. Biol.* **2002**, *318*, 733.
(6) Hustedt, E. J.; Beth, A. H. *Annu. Rev. Biophys. Biomol. Struct.* **1999**, *28*, 129.
(7) Larsen, R. G.; Singel, D. J. *J. Chem. Phys.* **1993**, *98*, 5134.
(8) Walter, E. D.; Sebby, K. B.; Usselman, R. J.; Singel, D. J.; Cloninger, M. J. *J. Phys. Chem. B* **2005**, *109*, 21532.
(9) Altenbach, C.; Oh, K. J.; Trabanino, R. J.; Hideg, K.; Hubbell, W. L. *Biochemistry* **2001**, *40*, 15471.
(10) Reddy, V. S.; Natarajan, P.; Okerberg, B.; Li, K.; Damodaran, K. V.; Morton, R. T.; Brooks, C. L., III; Johnson, J. E. *J. Virol.* **2001**, *75*, 11943.
(11) Kruse, J.; Hemminga, M. A. *Eur. J. Biochem.* **1981**, *113*, 575.
(12) Vriend, G.; Schilthuis, J. G.; Verduin, B. J. M.; Hemminga, M. A. *J. Magn. Reson.* **1984**, *58*, 421.
(13) Gillitzer, E.; Willits, D.; Young, M.; Douglas, T. *Chem. Commun.* **2002**, 2390.
(14) Štrancar, J.; Šentjurc, M.; Schara, M. *J. Magn. Reson.* **2000**, *142*, 254.
(15) Fox, J. M.; Zhao, X.; Speir, J. A.; Young, M. J. *Virology* **1996**, *222*, 115.
(16) Speir, J. A.; Bothner, B.; Qu, C.; Willits, D. A.; Young, M. J.; Johnson, J. E. *J. Virol.* **2006**, *80*, 3582.
(17) Adolph, K. W.; Butler, P. J. *J. Mol. Biol.* **1974**, *88*, 327.
(18) Adolph, K. W. *J. Gen. Virol.* **1975**, *28*, 179.
(19) Wang, L.; Lane, L. C.; Smith, D. L. *Protein Sci.* **2001**, *10*, 1234.
(20) Shi, J.; Koteiche, H. A.; McHaourab, H. S.; Stewart, P. L. *J. Biol. Chem.* **2006**, *281*, 40420.
(21) Margittai, M.; Langen, R. *Proc. Natl. Acad. Sci. U.S.A.* **2004**, *101*, 10278.